

Review

Review on Wearable System for Positioning Ultrasound Scanner

Lailu Li ¹, Lei Zhao ², Rayan Hassan ³ and Hongliang Ren ^{1,4,5,6,7,*}

¹ Department of Electronic Engineering, Faculty of Engineering, The Chinese University of Hong Kong (CUHK), Hong Kong

² College of Computer Science and Electronic Engineering, Hunan University, Changsha 410012, China

³ Department of Electrical and Computer Engineering, University of Pittsburgh, Pittsburgh, PA 15260, USA

⁴ Department of Biomedical Engineering, National University of Singapore (NUS), Singapore 119077, Singapore

⁵ Shun Hing Institute of Advanced Engineering, The Chinese University of Hong Kong (CUHK), Hong Kong

⁶ Shenzhen Research Institute, The Chinese University of Hong Kong, Shenzhen 518057, China

⁷ NUS (Suzhou) Research Institute, Suzhou 215000, China

* Correspondence: hlren@ieee.org; Tel.: +852-3943-8453

Abstract: Although ultrasound (US) scan or diagnosis became widely employed in the 20th century, it still plays a crucial part in modern medical diagnostics, serving as a diagnostic tool or a therapy process guide. This review provides information on current wearable technologies and applications used in external ultrasound scanning. It offers thorough explanations that could help build upon any project utilizing wearable external US devices. It touches on several aspects of US scanning and reviews basic medical procedure concepts. The paper starts with a detailed overview of ultrasound principles, including the propagation speed of sound waves, sound wave interactions, image resolution, transducers, and probe positioning. After that, it explores wearable external US mounts and wearable external US transducers applied for sonograph purposes. The subsequent section tackles artificial intelligence methods in wearable US scanners. Finally, future external US scan directions are reported, focusing on hardware and software.

Keywords: ultrasound scan; wearable; mount; soft robotic in ultrasound; PMUTs; CMUTs; AI in ultrasound



Citation: Li, L.; Zhao, L.; Hassan, R.; Ren, H. Review on Wearable System for Positioning Ultrasound Scanner. *Machines* **2023**, *11*, 325. <https://doi.org/10.3390/machines11030325>

Academic Editor: Huosheng Hu

Received: 20 January 2023

Revised: 20 February 2023

Accepted: 21 February 2023

Published: 24 February 2023



Copyright: © 2023 by the authors. Licensee MDPI, Basel, Switzerland. This article is an open access article distributed under the terms and conditions of the Creative Commons Attribution (CC BY) license (<https://creativecommons.org/licenses/by/4.0/>).

1. Introduction

In 1942, Dr Karl Theodore Dussik of Austria published the first paper on medical ultrasonics based on the research about transmission ultrasound examination of the brain [1]. Nowadays, ultrasound (US) imaging is a critical medical diagnostic technique to visualize soft tissues, such as muscles, blood vessels, joints, and internal organs, including pathological lesions, structure, and size of the targets [2–4]. The US corresponds to sound waves with high frequencies between 2 and 18 MHz, not detectable by the human ear [5]. It works by sending out mechanical waves that will be transmitted through soft tissues and reflected on tissue surfaces to the transducer. The latter is held by a probe positioned on the patient's body in a way that optimizes image quality. The following outstanding benefits of the US contribute to its widespread application in biomedical imaging throughout the years: safety due to the absence of cumulative biological adverse effects [6], as opposed to patient exposure to radiation in X-rays imaging method; non-invasiveness and non-destructiveness of this imaging method; portability, convenience and relatively low cost [7].

According to the purpose of the US scan, it could be grouped under three main categories (Figure 1): (a) External US scan. The most frequent targets of an external ultrasound scan are the heart or an embryo in the womb. The liver, kidneys in the abdomen, and pelvis can also be examined, including other muscles and limb joints. On the subject's skin, a portable probe is moved over the area of the body being inspected covered in

lubricating gel, which guarantees constant contact between the probe and the skin, and ensures easy movement of the probe. (b) Internal US scan. With the help of the internal scan, the physician can examine closely at internal organs. Images are then relayed to a monitor using a tiny ultrasound probe covered in sterile material. With the cutting-edge magnetic actuated capsule and microrobot technology, an untethered internal US scan may become a reality [8,9]. (c) Endoscopy US scan. To inspect bodily parts such as the stomach or esophagus, an endoscope is frequently put into the subject's mouth. In order to properly drive the endoscope down toward the stomach, the individual is often requested to lie on one side. An ultrasound device and light are attached to the endoscope, and sound waves are employed to produce pictures such as an external ultrasound.

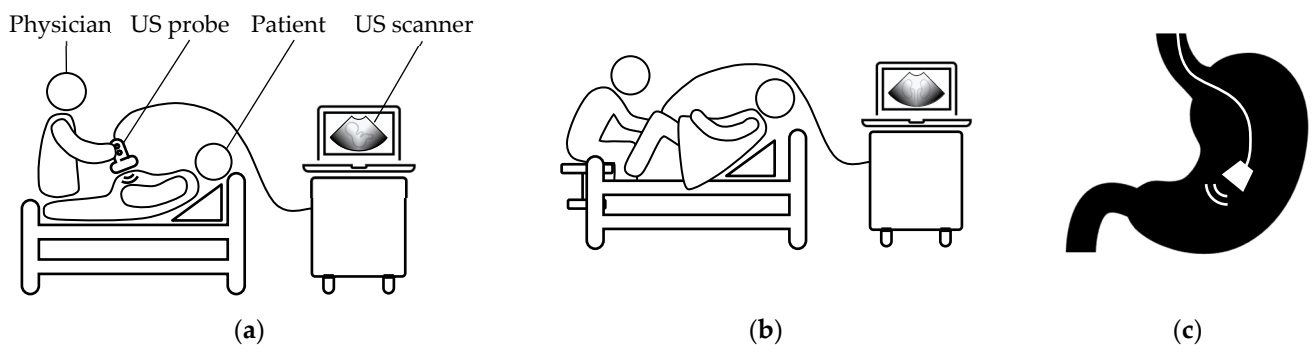


Figure 1. Classification of US scanners according to the purposes: (a) External US scan (Stationary US scanner); (b) Internal US scan; (c) Endoscopy US scan.

Although there are significant advantages of the external US scan, the following drawbacks also increase its implementation barrier: The waves have difficulty in traversing bones, especially in adults; The US method obtains poor image for a deep target, or when there is gas between the transducer and the target [10,11]; it relies on the trained operator with skill and experience, and this maximumly limits the use of the US imaging. In order to improve the usability and user-friendliness of the external US imaging apparatus and lower the learning and practice cost, robotic technologies have been introduced.

Robotic-assisted external US scanners could be classified into three groups according to the intervention level and manner of the robot [12,13], as shown in Figure 2: (a) Autonomous robot US scan, which offers reliable imaging without a physician, and this method is known as autonomous robotic ultrasound imaging; (b) human-machine collaboration US scan, which intends to bring a solution of quicker, more accurate, and more repeatable ultrasound imaging to physicians; (c) teleoperated US scan, which has the potential to address the issues such as the lack of trained specialists, increased travel and waiting time of the patient and sonographer, potential adverse effects on patient outcomes, and the physical strain of manipulating the probe experienced by doctors.

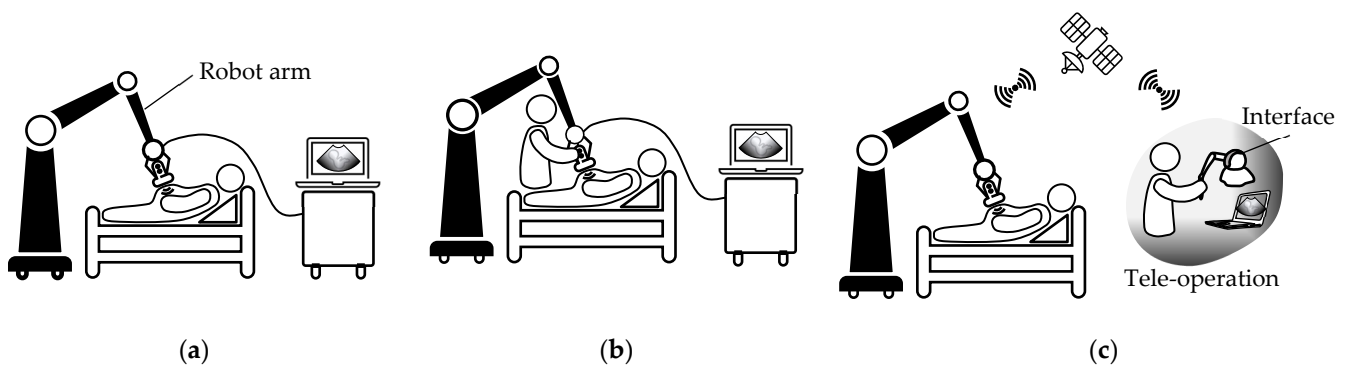


Figure 2. Classification of robotic-assisted US scanners according to the intervention level: (a) Autonomous robot US scan; (b) Human-machine collaboration US scan; (c) Teleoperated US scan.

Generally, the robot-assisted US scanner systems are a combination of the US probe and rigid commercial, custom-designed robot arms or parallel linkage mechanisms. According to mobility and wearability qualities, the robot-assisted US scanner systems could be categorized into three groups: stationary external US scanner (Figure 1a); portable external US scanner (Figure 3a), which is compact and, usually used together with a tablet or a mobile phone, could render an instant diagnosis for the subject without limitation of the sites; and wearable external US scanner (Figure 3b). Straps, rigid frames, and robotic technology are usually utilized. The wireless or wired wearable transducer could adhere to the skin of the subject, and continuous bio-information could be registered by it, which could be employed to track the performance of the subject. The importance of making point-of-care ultrasound (POCUS) a routine procedure that eventually all doctors can use in diagnosing patients is shifting the way of practicing medicine by enabling doctors to obtain critical information to supplement the conventional physical examination promptly. Von Haxthausen et al. [12] and Reza Monfaredi et al. [13] have conducted exhaustive reviews on the stationary rigid robotic assisted US scanners; check their publications for that type of US scanner. Yanick Baribeau et al. have presented an overview report of ultra-portable ultrasound apparatuses [14]. The scope of our paper will focus on the review of the wearable external US scanner.

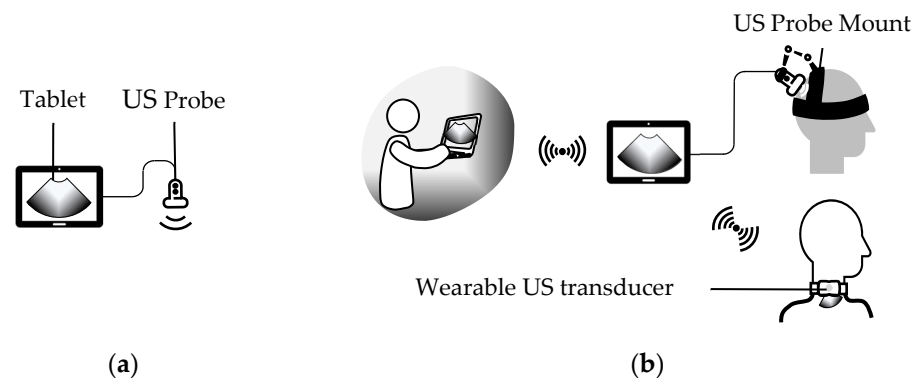


Figure 3. Classification of external US scanners according to the mobility and the ability to wear: (a) Portable US scanner; (b) Wearable US scanner.

We examine various combinations of the following keywords: Ultrasound, Wearable, Mount, Fixation, Transcranial Doppler (TCD), Common Carotid Artery (CCA), Echocardiography, Breast, Bladder, Thigh, Wrist, Calf, and Artificial Intelligent in the databases of Google Scholar, PubMed, IEEE Xplore Digital Library, and Science Direct.

This paper is an informative review of what has already been accomplished in wearable US scanners and is divided into five main parts: Section 2 explains the ultrasound principle; Section 3 covers different types of wearable apparatus implemented in US scanning, including wearable mounts and wearable transducers; Section 4 tackles artificial intelligence methods in wearable US scanner; Section 5 reports the future directions of wearable external US scanning; finally, we end with the conclusion.

2. The US Principles

2.1. Propagation Speed of Sound Waves

The propagation speed of sound waves depends on several factors, such as material density and compressibility [15]. The denser the material, the less sound propagates quickly. Similarly, the more compressible the fabric, the slower sound propagates, which can be represented by these equations: $c \propto \frac{1}{\sqrt{\rho}}$; $c \propto \frac{1}{\sqrt{\kappa}}$. c is the acoustic velocity in m/s, ρ is the density in Kg/m³ and κ is the compressibility [16].

Generally, the temperature does affect velocity, but since it is constant across the body, it would not be a contributing factor.

2.2. Sound Waves Interactions

Sound waves interact with tissues in several ways and are reflected back to the probe to display as an image. The parameter that is most influential in the process of obtaining ultrasound images is reflection, where sound waves are reflected after hitting a surface. The different densities of each surface tissue allow the US to distinguish between them. Therefore, each wave has a unique acoustic impedance z upon hitting a surface tissue, calculated by the following formula: $z = \rho c$. The acoustic velocity c is constant across the body. Thus, the acoustic impedance of most tissues is primarily a function of the tissue density ρ . An acoustic mismatch is created whenever waves hit adjacent regions with different densities, and sound waves are reflected by the mismatch [17]. The greater the mismatch, the more echoes are reflected back.

Consequently, ultrasound imaging is limited by the presence of bones and gas-filled structures. In fact, as sound is quickly transmitted through bones and poorly transmitted through air-filled structures [11], a high mismatch is created at bone and gas interfaces. Therefore, the transducer receives the majority of sound waves that are reflected. That limits the penetration of sound waves into deeper tissues and causes image artifacts. The percentage reflectivity of waves [18] is calculated using the following equation:

$$R = \left(\frac{z_2 - z_1}{z_2 + z_1} \right)^2 \times 100\%, \quad (1)$$

where z_1 and z_2 are the acoustic impedance of the tissues, R is the percentage reflectivity of waves. Then, the percent transmission T is calculated by $T = 100\% - R$.

Another important notion is refraction, where a certain percentage of reflected sound travels through the tissue and propagates toward other tissues [17]. That causes multiple challenges in ultrasound scanning, one of which is the detection of unwanted or inexact matters or substances on the retrieved images. Other equally essential mechanisms, such as diffraction, interference, and attenuation, also occur in the US.

2.3. Image Resolution

Resolution is the ability to distinguish two closely situated structures accurately. Axial resolution is the ability to differentiate between two close objects along the beam axis accurately. Higher frequency means better axial resolution [16]. However, there is a trade-off that must be made since depth decreases with increasing frequency because the signal becomes attenuated. On the other hand, the lateral resolution is the ability to differentiate between objects adjacent to one another that are perpendicular to the beam axis. The lateral resolution improves as the beam width decreases. Spatial resolution displays two objects close to one another as two separate images [19]. Finally, temporal resolution is the ability to distinguish two events in time [17]. It is determined by the number of image frames acquired per second (Hz).

2.4. Transducers

The primary function of the transducer is to convert the voltage into US and then reverse it. The two main types of US transducers are piezoelectric (PZT) transducers and capacitive transducers. The former is composed of a piezoelectric material that changes the shape of the piezoelectric crystal in response to an electric field, therefore exerting mechanical waves. The electrostatic fields between the conductive diaphragm and a backing plate are used in the latter transducers.

The idea of a diaphragm is also employed in micro-machined ultrasonic transducers (MUTs). These devices are constructed with microelectromechanical systems (MEMS) technology. The vibration of the diaphragm can be monitored or produced electronically by measuring the capacitance between the diaphragm and a closely spaced backing plate (CMUT) or by applying a thin coating of piezoelectric material to the diaphragm (PMUT) [20].

2.5. Probe Positioning

To obtain optimal image quality, the position of the probe is crucial. Two main factors should be taken into consideration, the contact force F between the probe and the patient, and the orientation of the probe [21]. Better quality is obtained when the angle between the sound waves and the normal direction θ of surface equals or approaches zero, which would ensure that most echoes are reflected back to the transducer.

The central axis of the probe and the normal plane need to be aligned. These vectors have two dimensions. First, an in-plane part \mathbf{A}_i and \mathbf{N}_i (Figure 4) aligned with the probe's front view, which corresponds to its wider side. Second, an out-plane component \mathbf{A}_o and \mathbf{N}_o (Figure 4), which is orthogonal to the in-plane component or aligned with the thinner sides of the probe [21]. Thus, it is important to have the angle of incidence close to zero. As for the contact force F , it is usually set to 3 ~ 15 N [21]. If F is too large, the image quality declines due to deformations.

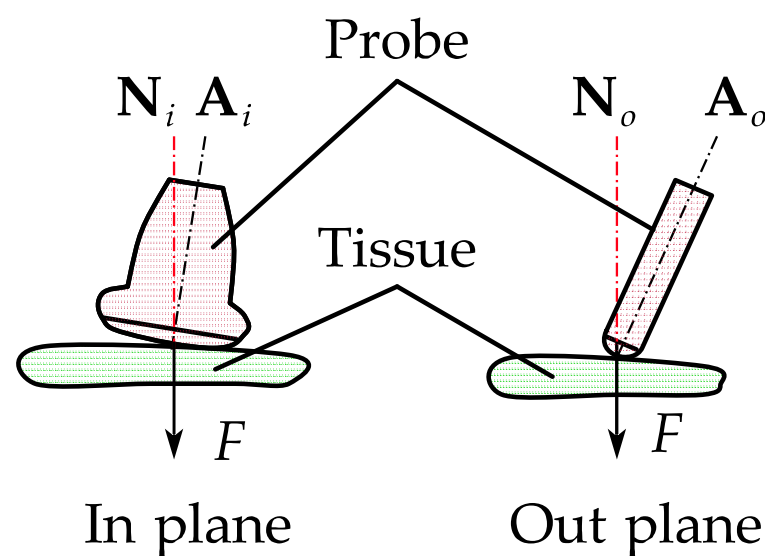


Figure 4. US images; in-plane and out-plane view.

Consequently, the positioning of the probe should be taken seriously, as it highly affects the quality of the obtained images. Therefore, with robotics taking over and handling the probe, it is vital to study the transducer's orientation.

3. Wearable External US Scanner

Biosignals that acquire real-time and long duration could reveal a lot of vital information about the physiological status of the subject. For decades, scientists and researchers have been focusing on the research to transfer the conventional US scan into a wearable US scan system.

As shown in Figure 5, the wearable external US scanner can be classified into two main categories: transducer mount and wearable transducer. Indeed, they can also be organized by the specific organ or tissue they could be applied to (Figure 6). In this section, we examine these two components: wearable external US probe mounts and wearable external US transducers.

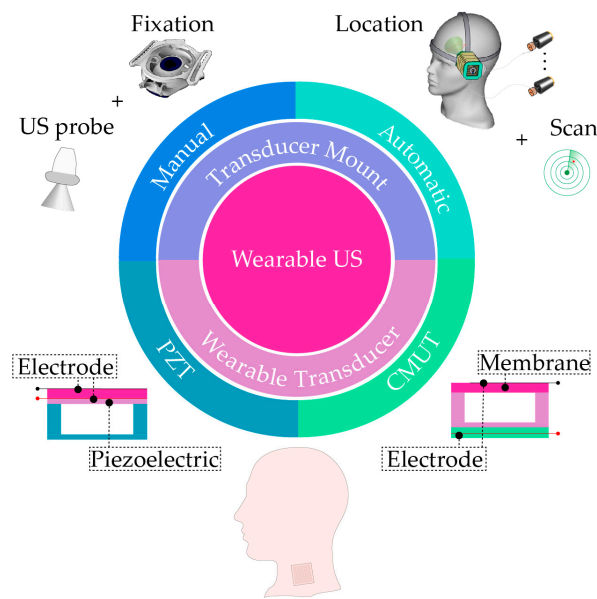


Figure 5. Classification of the wearable US scanners.

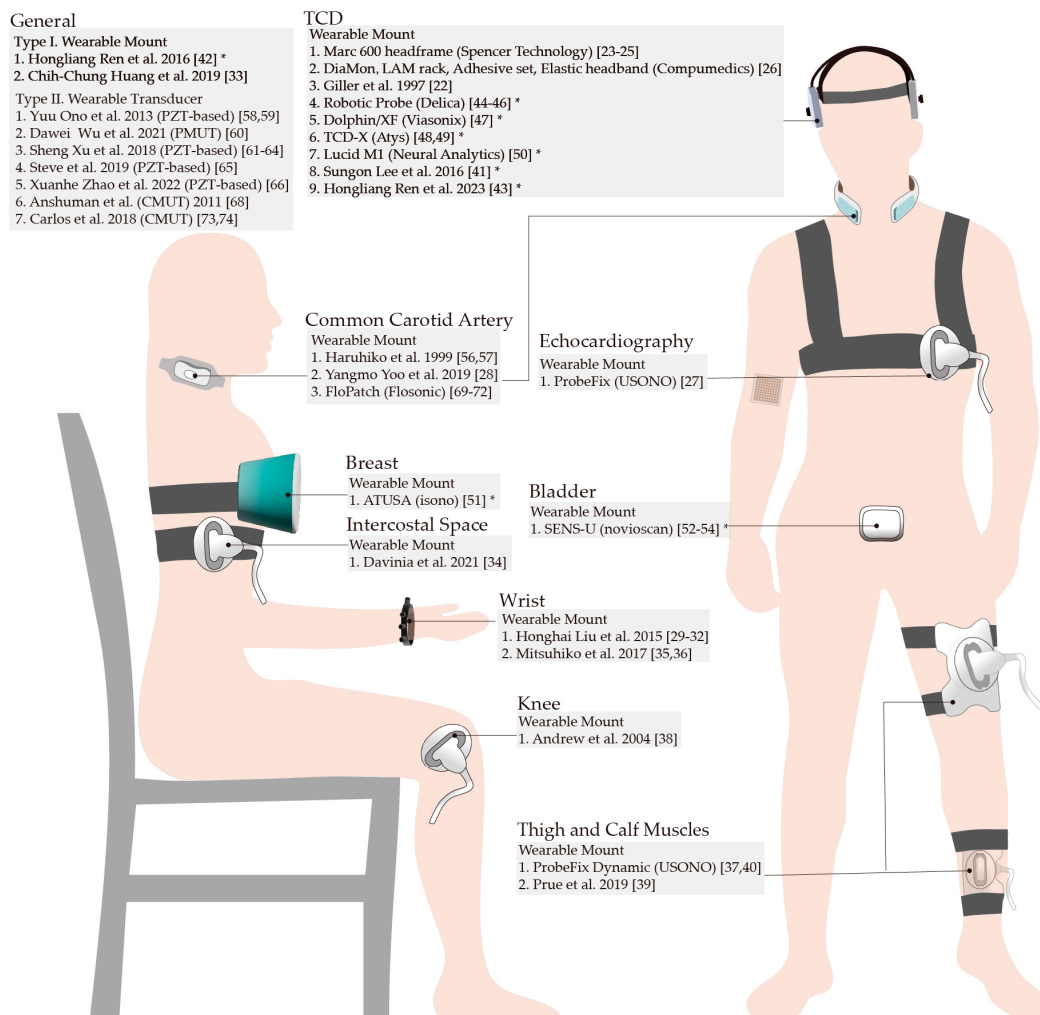


Figure 6. Overview of current wearable US scanners by the specific applied organ. (“*”: Autonomous US scanner).

3.1. Wearable External US Transducer Mounts

A wearable external US probe mount is the most common solution, combining a conventional commercial probe and a wearable mount. The wearable mounts are compatible with existing devices in hospitals and clinics. Transducer fixation, rigid parallel linkages, soft pneumatic actuators, and origami-based mechanisms are generally used in mountable external US scanners. Some could actively hold and move the commercial transducer to search and scan the targeted region of interest (ROI). Thus, the mounts can be categorized into two types according to the operation manners: manual (Table 1) and autonomous (Table 2).

- Manual External US Transducer Mounts

For a validated sonography analysis, the field of view (FOV) must remain immobile during the whole measurement procedure in dynamic ultrasound scan applications. The most straightforward and inexpensive solution is to fix the transducer in the specified positions.

For the supervision of head bio-information, Giller et al. developed a probe fixation for TCD Ultrasound [22]. The ROI is first marked, a thin plastic then placed over the subject's temporal, a ceramic shell is used to set the TCD probe, and the polymer material is injected through the holes of the shell. After curing, the device is strapped on the head with elastic tape. Once the device is fabricated, it can only be used for personal specific area scans. In the meanwhile, the angle is unadjustable. Curing the polymer material requires time, and the position and penetration angle of the transducer can be influenced to a great extent by other disturbances during that process. Marc 600 in Figure 7a (Spencer Technologies, Medway, MA, USA) is a US head mount combined with the ST3 TCD system (Spencer Technologies, USA) to provide a securable and adjustable TCD probe head mount for unilateral or bilateral monitoring [23–25]. Australian company Compumedics offers four probe fixations for continuous long-term bilateral recordings in TCD monitoring LAM rack, Elastic headband, Adhesive set, and size-adjustable DiaMon [26].



Figure 7. Wearable mounts: (a) Marc 600; (b) ProbeFix in echocardiography [27] (open access).

Fixations could be adopted in the scan of the trunk and upper limb organs, including the CCA, cardiac, and wrist. Transducers installed in a ring-like frame are frequently employed for ultrasound imaging of the wrist and common carotid artery. Yangmo Yoo et al. created a wireless neckband US scanner for constantly monitoring blood flow dynamics [28]. It uses two 2.5-MHz commercial US transducers to collect Doppler data from both carotid arteries. Honghai Liu et al. reported a wearable US band for the forearm, a non-invasive way to detect morphological muscle deformation [29,30]. The band utilizes multiple commercial low-profile US transducers. By analyzing the echo patterns, the sonography principles can identify the intended motions of the fingers. They also propose offline and online algorithms for hand gesture recognition with high accuracy [31]. A real-time hand and wrist predictive algorithm is introduced by analyzing the US sensing information [32]. Chih-Chung Huang et al. developed a portable US scan system using a low-profile transducer [33]. To measure the diagram thickness during rehabilitative ultrasound imaging (RUSI), a support fixation is utilized [34]. The device uses a thoracic orthotic to hold the US probe to ensure measurement accuracy. During the monitor procedure, the subject must lie flat on the bed and keep as much as possible in a fixed position, as

the body movement may cause an error. To assess the biomechanical efficacy of carpal tunnel release (CTR) for carpal tunnel syndrome (CTS), Mitsuhiko et al. also used this concept to construct a fastening device to attach the US transducer perpendicular to the subject's wrist without exerting too much compression [35,36]. Identically, the subject must hold the wrist to remain motionless in use. USONO, a Dutch company, focuses on developing ultrasound probe mounts to make the US more accessible to operators. Their products of the ProbeFix Dynamic series support dynamic movement-related ultrasound measurements, as presented in Figure 7b. It secures an ultrasound probe, immovable to the ROIs [27,37].

For the scan of the lower limb, a similar custom-designed apparatus, a patellar probe holder, was developed by Andrew et al. to acquire knee information during movement [38]. Another customized holder is also designed for measuring tendon elongation [39]. However, contact between the transducer and the skin is occasionally lost, leading to signal loss and low-quality scan imaging [38,40]. The risk of the too tightly strapped transducer could be as much of an issue as strapping too loose, raising a potential impact on tissue behavior and perfusion by the compression [37].

Table 1. Wearable External US mounts (Manual) ¹.

Name	Solution	Body Part	Application	Level	Ref
Giller et al., 1997	Fixation, Adhesion	Head	TCD	Custom	[22]
Marc 600	Fixation	Head	TCD	Commercial	[23–25]
DiaMon					
LAM rack, Adhesive set, Elastic headband, Yangmo Yoo et al. 2019	Fixation, Strap and Adhesion	Head	TCD	Commercial	[26]
Chih-Chung Huang et al., 2019	Neckband	Neck	CCA	Custom	[28]
Honghai Liu et al., 2015	Low profile Transducer	General	General	Custom	[33]
Davinia et al., 2021	Band	Wrist	Gesture Prediction	Custom	[29–32]
Mitsuhiko et al., 2017	Fixation, Strap	Intercostal Space	RUSI	Custom	[34]
ProbeFix series	Fixation, Strap	Wrist	CTR assessment	Custom	[35,36]
Andrew et al., 2004	Fixation, Strap	Cardiac, Limb	Muscle scan, Echocardiography	Commercial	[27,37,40]
Prue et al., 2019	Knee brace	Knee	Patellar position	Custom	[38]
	Fixation, Strap	Low limb	Achilles strain	Custom	[39]

¹ Although the subject can freely move within a specific range under these manually operated US mounts, unsteady continuous monitoring may be caused.

- **Autonomous External US Transducer Mounts**

Motor-actuated linkage mechanisms are frequently adopted because they typically have high controllable accuracy and low cost. A wearable device with a two-degree of freedom (DOF) parallel spherical five-bar linkage described in [41] is intended for the non-invasive transcranial US simulations. The device fixes the simulator around the head. It also has a three-DOF serial arm, exerting a five-DOF motion on a human head. The latter is used to control the simulation angle and depth. However, the bulky weight of the linkage mechanism limits its practical application.

The development of robots for US scanning purposes is limited to rigid structures. That affects their flexibility and makes it complex for engineers to ensure compliance. To improve the performance of the probe mount, the creation of soft robots has been widely exploited. Soft robotics is a field that involves the design and fabrication of robots made out of compliant material. That allows the production of robots to take a wider variety of shapes and for the robots to perform more tasks, making medical procedures more accessible and efficient. Hongliang Ren et al. presented an attachable and portable soft robot that can optimize probe positioning and contact force [42]. The device (Figure 8a) consists of three main parts. The suction cups are used to attach the device to the body using a vacuum suction force of 50 N. The support structure comprises a top plate with one soft

pneumatic actuator in each of the four quadrants, a bottom plate with four quadrants that work independently, and holes that attach to the suction part. Finally, the soft pneumatic actuators can be applied to steer the US probe. Over-COM is an overhead collapsible origami-based mount that could hold a TCD ultrasound probe that registers Cerebral Blood Flow Velocity (CBFV) for early ischemic stroke detection (Figure 8b) [43]. The Over-COM consists of a system that is placed onto the temporal window of the patient. It includes the TCD probe, which is attached by eight strings, four of which are attached to the top plate of the probe holder and four to its bottom plate. It contains straps that hold all the wires and string sheaths connecting to an external unit with the microcontroller, eight rotary motors, and a battery away from the patient's head. The actuators allow for 4 DOF ensured by the probe holder, which exerts rotation about the roll and pitch axes. Another DOF is secured along the vertical axis perpendicular to the skin plane.

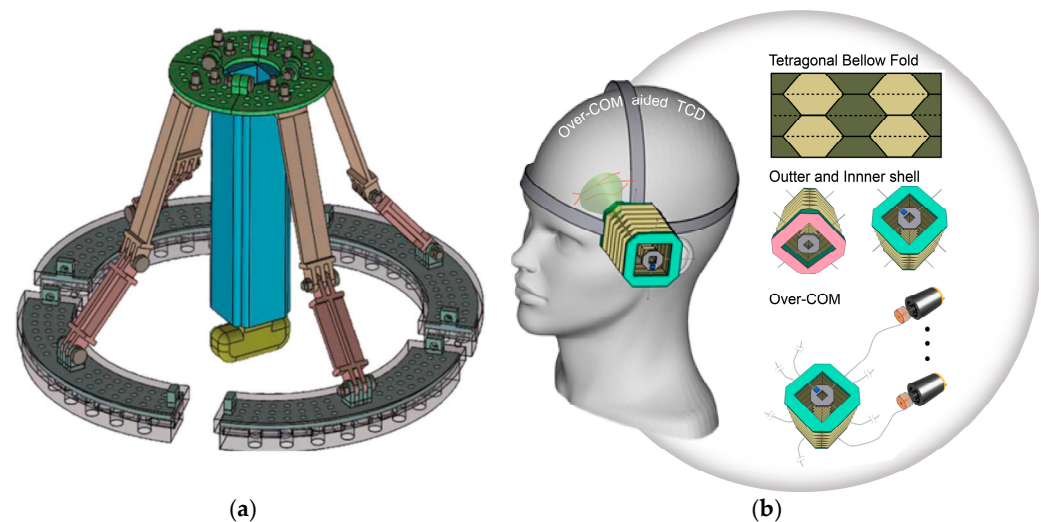


Figure 8. Soft robotic combined wearable US: (a) Pneumatic actuated wearable US probe mount [42] (reproduced with permission); (b) Over-COM [43] (open access).

The Robotic Probe developed by Delica (Shenzhen, China) allows continuous prolonged monitoring of the middle cerebral artery (MCA) CBFV shown in Figure 9a. The system adapts robotically controlled probes with auto-adjustment algorithms for probe shift [44–46]. The system could achieve a scan depth of 5–150 mm. Dolphin/XF (Viasonix, Israel) is also a robotic TCD machine for patient assessment with autonomous bilateral brain scan, identification, and self-stabilization [47]. TCD-X [48,49] is a portable real-time TCD signal recording device developed by the collaboration between Atys medical (France) and Dr. Rune Aaslid, who first introduced the TCD. The Lucid M1 system (Neural Analytics, USA) is an intelligent TCD platform with a scan depth capability of 23 to 151 mm, and auto cerebrovascular reactivity calculations [50].

The Food and Drug Administration (FDA) of the United States has approved the wearable ultrasound system ATUSA of iSono Health (South San Francisco, United States) [51], which is a portable and AI-driven autonomous 3D breast ultrasound scanner and is intended for personalized breast imaging. The ATUSA scanner automatically records the whole breast volume, enabling reproducible breast ultrasound imaging at the point of service without requiring a professional ultrasound operator. The innovative scan process of ATUSA provides clinicians with superior 3D visualization at their fingertips, allowing them to develop confidence in their diagnosis and patient monitoring.



Figure 9. Autonomous wearable US: (a) Robotic Probe [46] (open access); (b) SENS-U [52] (reproduced with permission).

SENS-U (Figure 9b) is a small, Bluetooth-connected, battery-operated ultrasound equipment [52–54]. A double-sided adhesive and regular ultrasound gel are used to affix the SENS-U on the lower abdomen. The SENS-U uses four ultrasonic transducers in tandem to send ultrasound waves vertically to the abdominal wall in the direction of the bladder within a 30-degree FOV. The internal programming of the SENS-U compares the received ultrasonic reflection with a maximum amplitude of the reflection-based threshold to automatically calculate the axial position of the anterior (AW) and posterior (PW) bladder walls. The individual bladder filling state is calculated based on a predetermined threshold for the average anterior–posterior (A-P) bladder dimension.

Table 2. Wearable External US mounts (Automatic) ¹.

Name	Solution	DOF	Dimensions	Weight	Body Part	Application	Level	Ref.
Sungon Lee et al., 2016	Linkage	5	-	-	Head	TCD	Custom	[41]
Hongliang Ren et al., 2016	Soft actuator	Linear motion Single plane Semi-circle	-	-	General	General	Custom	[42]
Hongliang Ren et al., 2023	Origami	5	-	-	Head	TCD	Custom	[43]
Robotic Probe	Headframe	-	10.5 × 6 × 2 cm	55 g	Head	TCD	Commercial	[44–46]
Dolphin/XF	Headframe	-	8.5 × 7.5 × 3.5 cm	126 g	Head	TCD	Commercial	[47]
TCD-X	Headset	-	-	-	Head	TCD	Commercial	[48,49]
Lucid M1 with headset	Headframe	-	-	-	Head	TCD	Commercial	[50]
ATUSA	Strap	-	-	-	Breast	Breast US	Commercial	[51]
SENS-U	Adhesion	-	-	-	Abdomen	Bladder US	Commercial	[52–54]

¹ The subject can freely move within a specific range; steady, continuous monitoring can be achieved by virtue of autonomy. (“-”: Not Applicable.)

3.2. Wearable External US Transducers

The other type of wearable US scanner applies an external US transducer that could be attached to the human body and realize continuous supervision of ROI. Thus, several novel recreated external US transducers with improved aspects of small, portable, and wearable advantages have been developed using piezoelectric (PZT-based, PMUT), CMUT, and soft robotics technologies. A summary of the wearable transducer is presented in Table 3. For the materials and fabrication process of the wearable external US transducer, refer to the work of Lawrance [55].

Haruhiko et al. proposed a wearable ultrasound doppler necklace to monitor blood flow [56,57]. The apparatus comprises a number of piezoelectric transducers mounted at the neck that produce various ultrasonic beams pointed at the common carotid artery. The centreline velocity of the artery is then reconstructed, together with an estimate of the

velocity profile and other physiological characteristics, using the Doppler frequency shift caused by the flowing blood.

To observe skeletal muscle contraction, Yuu Ono et al. created a wearable and flexible ultrasonic sensor [58]. The sensor is built using a polyvinylidene fluoride (PVDF) piezoelectric polymer film. Less than 1 g in weight, 200 μm in thickness, and flexibility make this sensor wearable and allow for non-invasive, continuous muscle monitoring without impeding muscle movement, which is impossible with a traditional handheld ultrasonic probe. The created sensor tracks muscle contractions in the forearm and index finger using through-transmission and ultrasonic pulse–echo measurements. The sensor with an active area of 15 mm \times 15 mm in the pulse–echo mode achieved 23 mm ultrasound penetration depth in the lower leg of a human subject [59].

Through an enhanced, straightforward, and reliable adhesive bonding fabrication approach, a flexible piezoelectric micromachined ultrasonic transducer (PMUT) array with bending mode functionality has been conceived and created by Dawei Wu et al. [60]. The 3 \times 3 element flexible PMUT array has been designed with a resonance frequency of approximately 161 kHz. Their device, which achieves an output signal of 75 mV_{pp} under 100 V_{pp} stimulation, may be manufactured on various flexible substrates and adhered to concave, convex, and undulant surfaces.

Sheng Xu et al. from the University of California at San Diego proposed a stretchable transducer array that could be applied on complex surfaces [61,62]. Additionally, their team described an ultrasonic transducer patch for continuous monitoring of many indicators [63]. It also provides mechanical robustness and flexibility while adhering to curved skin surfaces. Then, to continually monitor the deep tissues (14 cm), they proposed a flexible wearable US transducer for specific tissues [64]. The gadget enables active focusing and directing of ultrasound beams across a variety of incidence angles to target regions of interest.

Steve et al. described an ultrasound patch with integrated imaging and modulation modes for image-guided neural therapy. For the purpose of localizing nerves, an array of PZT-based transducers with mechanical flexibility and a 5 MHz resonance frequency was developed [65].

Xuanhe Zhao et al. described a bioadhesive ultrasound (BAUS) device comprising a thin, rigid ultrasonic probe firmly attached to the skin using a couplant constructed of a flexible, resilient, bioadhesive, hydrogel–elastomer hybrid [66]. The structure of BAUS is presented in Figure 10. Various abdominal organs can be maximumly monitored for two days using the BAUS. The BAUS gadget might make it possible for numerous diseases to acquire diagnostic and monitoring tools. The performance of the BAUS probes is better than those of the wearable ultrasound devices [37,40,64,67].

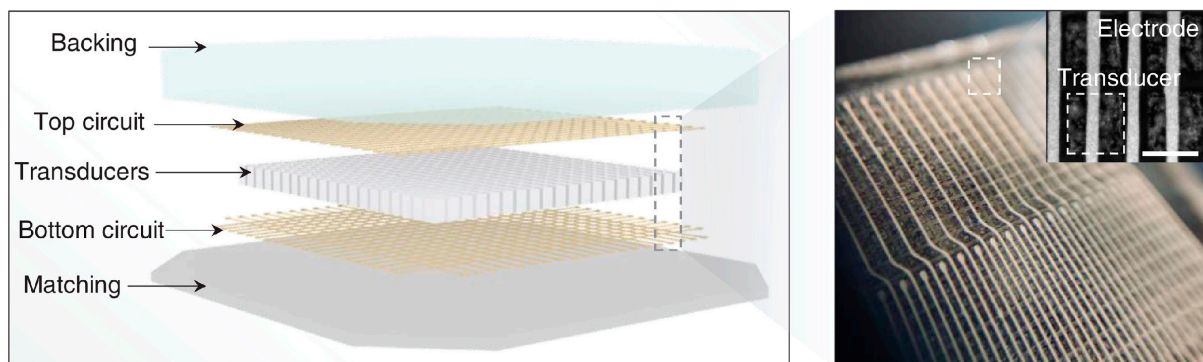


Figure 10. The structure of BAUS [66] (reproduced with permission).

Anshuman Bhuyan et al. provided a discreet, wearable ultrasonic probe that could be applied to a patient’s body and used to periodically or continuously monitor organ function [68]. CMUT with a 64-element 1D array running at 5 MHz constitutes the probe. The finished construction has dimensions of 6 \times 3.5 \times 0.35 cm. The probe is connected

to a backend system that transmits high voltage pulses and digitizes the data from RF echoes received to reconstruct images. The imaging tests conducted on a human neck and a commercially available phantom show that the CMUT probe provides equivalent picture quality to the commercial probe.

Jon-Émile S. Kenny et al. developed a wearable, wireless, continuous hands-free ultrasound patch (Flosonics Medical, Sudbury, ON, Canada) for quantitative doppler monitoring in the carotid artery [69]. The patch is constructed with two continuous-wave 4 MHz ultrasound transducers, one is for continuously transmitting sound, and the other for receiving echoes. It is attached to the neck and uses an automated algorithm to measure doppler blood flow parameters in the common carotid artery with a 4 cm penetration depth [70,71]. The patch works well with the Flopatch App, which can run on a tablet [72]. This device assists doctors in quantifying hemodynamic changes in response to an intervention.

An array of CMUT was created by Carlos et al. for sonograph [73]. A considerably lower manufacturing cost using inexpensive materials that preserve or improve present sensitivity is required for widespread usage of CMUTs [73,74]. They proposed a novel manufacturing procedure for polymer-based CMUTs (polyCMUTs) employing the photopolymer SU-8 and Omnicoat [75]. This low working voltage and great device sensitivity can be ascribed partly to a pre-biasing state on the membrane. They demonstrated that SU-8 might be utilized to reduce the cost of CMUTs by combining a unique sacrificial layer with a top electrode implanted inside the membrane.

Table 3. Wearable US Transducer ¹.

Name	Solution	Penetration Depth	Operating Frequency	Application	Level	Ref.
Haruhiko et al., 1999	PZT-based	14 mm	4 and 8.1 MHz	CCA	Custom	[56,57]
Yuu Ono et al., 2013	PZT-based	23 mm	2.2 MHz	General	Custom	[58,59]
Dawei Wu et al., 2021	Flexible PMUT	140 mm	2 MHz	General	Custom	[60]
Sheng Xu et al., 2018	PZT-based	140 mm	2 MHz	General	Custom	[61–64]
Steve et al., 2019	PZT-based	20 mm	5 MHz	General	Custom	[65]
Xuanhe Zhao et al., 2022	PZT-based	60 mm	3, 7, and 10 MHz	General	Custom	[66]
Anshuman et al., 2011	CMUT	50 mm	5 MHz	General	Custom	[68]
FloPatch	Continuous Wave Transducer	40 mm	4 MHz	CCA	Commercial	[69–72]
Carlos et al., 2018	CMUT	85 mm	5.8 MHz	General	Commercial	[73,74]

¹ The subject can freely move; steady, continuous monitoring can be achieved.

4. Applications of Artificial Intelligence in Wearable US

Aside from being outfitted with advanced hardware technologies such as communication modules and networks, US wearable systems have the potential to utilize artificial intelligence (AI) methods to carry out various tasks. Generally, AI can be defined as a compound system to simulate the human cognitive process, which involves learning, applying and dealing with complex situations. Two primary application fields of AI have been identified to boost the autonomy of US wearable systems in recent years: image understanding and robot navigation, such as navigation enhancement in landmark detection [76], auxiliary diagnosis in lesion areas detection [77], or individual customization in optimal therapy [78]. AI is the overarching field that encompasses machine learning (ML) and deep learning (DL). ML is a subset of AI focusing on algorithms learned from data, which covers the ability of a system to learn about data using supervised or unsupervised, semi-supervised ML methods and reinforcement learning (RL). DL is a subset of ML that uses neural networks to process data and make predictions. This section discusses the hierarchical relationships and context of AI, ML and DL, as shown in Figure 11. The following section introduces the development trend of AI-based US wearable systems in recent years, according to the different AI techniques such as supervised learning, unsupervised learning, semi-supervised learning, RL and DL.

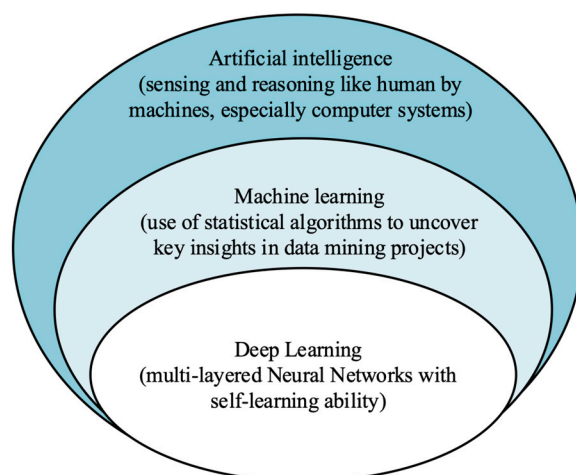


Figure 11. The hierarchical relationships and context of artificial intelligence.

4.1. Supervised Learning

In supervised learning, the explicit labels of datasets typically labeled by experts are referred to as “ground truth”. The goal of the supervised learning algorithm is to minimize the gap between the ground truth and the predicted values. Based on a class-weighted support vector machine (SVM), Chao et al. [79] proposed a portable wireless photoplethysmography sensor to assess the health of arteriovenous fistula. Zhao et al. [80] presented a wearable system combining accelerometers and machine learning algorithms to monitor fetal movement automatically. Mesbah et al. [81] proposed a novel algorithm using the random forest algorithm for automatic fetal movement recognition by collecting data from wearable tri-axial accelerometers placed on the maternal abdomen. Supervised learning is an effective tool in classification, characterization and regression tasks, but data annotation for specific medical applications is highly time-consuming and experience-dependent. Therefore, it is necessary to reduce the dependence on labeled data from large-scale images, and develop AI-based US wearable systems more efficiently [82].

4.2. Supervised Learning

Supervised learning requires expert annotations and is correspondingly labor-intensive and expensive. In contrast to supervised learning, unsupervised learning could identify the intrinsic structure of unlabeled input data by similarities or clusters. Yang et al. [32] designed a novel subclass discriminant analysis algorithm with an unsupervised strategy for predicting wrist rotation and finger gestures via US wearable system. Abhishek et al. [83] proposed a point-of-care US imaging assembly to perform unsupervised monitoring of body parts for early detection of cancerous growths. Unsupervised learning provides a low-cost and powerful alternative solution to overcome the need for large-scale unlabeled data. However, US wearable systems based on unsupervised learning have yet to be extensively evaluated in clinical application.

4.3. Semi-Supervised Learning

Semi-supervised learning algorithms play an essential role when the number of labeled samples is few but the number of unlabeled data is significant. In this situation, supervised and unsupervised learning cannot work effectively. Hou et al. [84] implemented the semi-supervised convolutional neural network based on successive subspace learning for breast US image classification, and achieved on-device training. However, only a few prior arts explore semi-supervised learning in the wearable US system domain. Further exploration is needed to explore whether semi-supervised learning with limited labeled images can achieve satisfactory performance.

4.4. Reinforcement Learning

In reinforcement learning (RL), data labels are obtained from the interaction of a dynamic environment rather than by explicit learning. The computer receives either positive or negative RL feedback in a dynamic environment, and the RL algorithm correspondingly receives reward or penalty feedback to output the expected results. Like a hybrid of supervised and unsupervised learning, RL leads to a breakthrough in autonomous robot navigation, such as human-aware path planning [85], object manipulation [86], and obstacle avoidance in complicated dynamical environments [87]. Some researchers utilize imitation learning techniques, such as inverse reinforcement learning [88] and behavioural cloning [89], to complete the probe navigation learned from expert demonstrations. Jarosik et al. [90] designed an RL agent to move a virtual probe in a simplified static environment, but the real-world probe navigation task is much more challenging due to the complicated situations of different patients. Similarly, Hase et al. [91] used RL to learn cardiac US probe navigation in a simulation environment built by projecting a grid on subjects' chests. Since the simulation environments are constructed with a limited number of US probes, the learned actions are restricted to the collected data. Additionally, assuming the patient is in a static state relative to the probe is too ideal for performing actual US scanning.

4.5. Deep Learning

Deep learning is a significant subset of machine learning, defined by non-programmed learning from a large amount of data with the convolutional neural network (CNN). Recently, CNN has shown outstanding performance in image recognition and raw data processing [92,93], which makes it a potential tool for US image analysis and reduces variation factors of US scanning. In particular, computer-aided systems in US analysis have already been recognized by the industry and benefited a lot from some primary applications, shown in Figure 12, such as (1) detection: automatically recognizing organ structures, lesions, and other regions of interest [94]; (2) classification: analyzing US images to check disease status or sort it into a certain category [95]; (3) segmentation: delineating the precise boundaries of object areas [96]; (4) other applications, including image registration, 3D reconstruction and image denoising [97–99]; etc. Nevertheless, a typical DL application can easily exhaust wearable device resources owing to a large amount of multiply, accumulate and memory access operations. Though the more resource-consuming training phase can be offloaded onto high-performance-computing-powered mainframes, the inferencing phase forwards urgent demand for DL-based deployment in US wearable applications. Therefore, managing energy consumption and achieving the expected performance is one of the projects worth studying in the future.

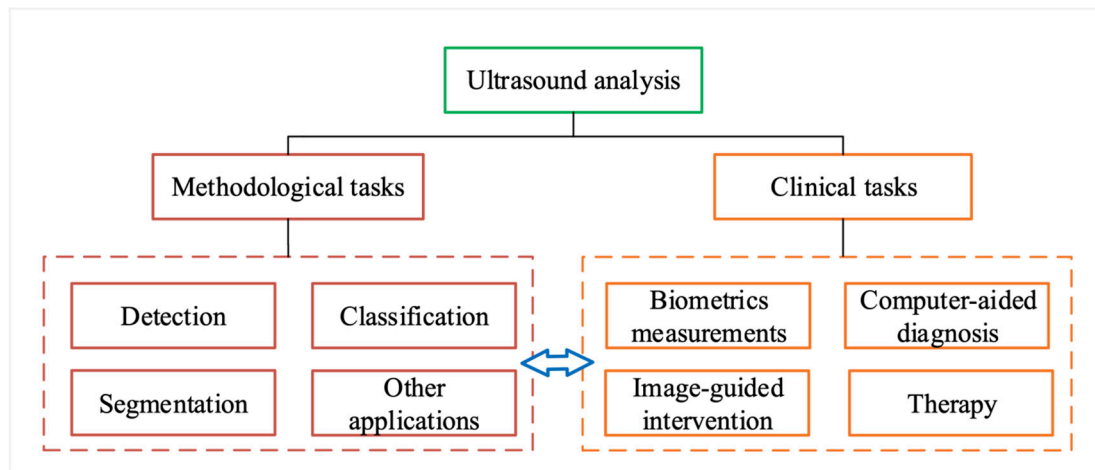


Figure 12. Summary of the deep learning applications in US image analysis according to methodological and clinical tasks.

5. Future Directions of Wearable External US Scan

In our review of wearable external US scanners, we focus on the previous studies that have been used or are intended for application in human bio-information acquisition. However, we do not include the ultrasound equipment used for industrial scenarios that could possibly be transferred to medical applications [100]. Although the current existing human body wearable US scanners could cover most situations, they still need to be improved for further medical monitoring.

- Issues with existing apparatuses

The wearable US probe fixation works well with the existing US system in the hospital and clinics. An autonomous mount could render an adjustment of the US penetration angle. However, the volume is bulky, critically affecting the movement of the subject, and causes an uncomfortable feeling in the user. In the meantime, because the systems should be utilized in conjunction with traditional US scanners, it is challenging to achieve wireless information transmission. Consequently, this also brings limitations to continuous supervision. The contact between the transducer and the skin is occasionally lost, which leads to the loss of the signal. Even worse is the case with the manually operated mount, because the probe cannot be autonomously adjusted. However, a bigger pre-load between the transducer and the tissue may cause the unnatural performance of the tissue. Although the soft autonomous US probe mount perfectly comforts the subjects with a relaxed and low-stress self-scan, it still faces the challenges of tethered US scanners or tethered commercial transducers.

The recreated US transducers fabricated by MEMS technology are lightweight and could well adhere to the desired body parts of the subject to achieve continuous monitoring. The stretchable feature enables the transducers to align roughly with the deformation of the body tissue. However, the penetration angle of the sound wave is also affected by the deformation of the tissue and the displacement between the body tissue and the transducer. Even the posture change of the subject could exert extreme variation in the penetration angle. Most of the existing recreated transducers encounter the same challenge as the wearable probe mounts, which are not wirelessly available.

- Future Trends in Hardware

The future wearable external US scanner should clear up the following challenges: wireless information transmission and fixed penetration angle relative to the ROIs. The solution proposed by Jon-Émile S. Kenny et al. [68] could be adopted to realize wireless data transmission through Bluetooth. The MEMS transducer possesses incomparable advantages in wearability and portability. In turn, to ensure the US penetration angle

and a better feeling of wearing, a combined solution of the MEMS transducer and soft pneumatic or origami-based mount is the best. Thus, with the help of the soft mount, the accuracy of the US scan could be enhanced. Pneumatic or origami-based structures may provide elasticity benefits to the skin while achieving vibration isolation and dampening for active movement. In order to realize a long duration of continuous monitoring, a way to provide the power supply should be developed. It is desirable to have a robust energy supply device that is portable, small and has a high energy density. The recently developed devices harvesting human-based mechanical and thermal energy demonstrate the potential to power sensor systems.

- **Future Trends in Software**

With the emergence of US diagnostic and 5G wireless transmission technologies, these advanced technologies provide powerful network services to support “real-time” interaction of digital imaging and offer a great opportunity for the development of AI technology. Wearable US systems provide monitoring and scanning features such as biofeedback or other sensory physiological functions. For example, Lammie et al. designed a wearable seizure warning system for patient-specific settings by combining the deep learning model with neuromorphic hardware [101]. The trend of wearable US systems will continuously advance toward multifunctional, lightweight, self-sustainable, and explainable AI systems.

Localizing targeted areas of interest has always been up for research. Computer-aided diagnostic (CAD) systems should be developed to locate and distinguish ROIs. Artificial Intelligence (AI) is a crucial concept for determining the exact ROIs to scan based on the model’s characteristics. The algorithm compares the live US images to predisposed pictures of the same tissue used for the same scanning purposes and predicts the exact scanning area. Previous studies involving AI use for localization purposes are reported by Jialin Zhu et al. [102] and Mehran Pesteie et al. [103], while further research to improve efficiency and accuracy should be conducted. The trend of wearable US systems will continuously advance toward multifunctional, lightweight, self-sustainable, and explainable AI systems.

6. Conclusions

In conclusion, ultrasound has opened doors for numerous applications in the medical field. It is used to monitor organs and tissues, detect tumors or infections, or even target specific locations for drug delivery. None of these practices would have been possible without the fabrication of robotic systems that help guide these procedures. With the development of wearable soft robots and MEMS technology, applications are limitless, such as the development of pneumatic, origami-shaped devices; US transducer patches are quickly emerging on the market, and many medical applications are expanding. However, in order to comfort in external US scanning operations to meet the increasing requirement for both doctors and patients, further study should be conducted in both hardware and software to eliminate the need for the sonographer to be present on site. Human assistance will slowly fade away for specific tasks, with the US scanning moving towards autonomous functioning. The wearable US scanning technology will enhance the ability of a clinician to accurately prescribe medicine for patients, long-term monitoring of human physiological indicators, and emergency detection.

Author Contributions: Conceptualization, H.R., L.L. and R.H.; methodology, L.L., L.Z. and R.H.; formal analysis, L.L. and L.Z.; investigation, L.L., L.Z. and R.H.; resources, L.L., L.Z. and R.H.; writing—original draft preparation, L.L., L.Z. and R.H.; writing—review and editing, H.R., L.L. and L.Z.; visualization, L.L. and L.Z.; supervision, H.R.; project administration, H.R.; funding acquisition, H.R. All authors have read and agreed to the published version of the manuscript.

Funding: This research was funded by the National Key R&D Program of China under Grant 2018YFB1307700 (with subprogram 2018YFB1307703) from the Ministry of Science and Technology (MOST) of China, the Shun Hing Institute of Advanced Engineering (SHIAE project #BME-p1-21, 8115064) at the Chinese University of Hong Kong (CUHK), the Key Project 2021B1515120035 of the Regional Joint Fund Project of the Basic and Applied Research Fund of Guangdong Province, Singapore Academic Research Fund under Grant R397000353114, Health Longevity Catalyst Awards HLCA/E-403/22 by NAM & RGC, Shenzhen-Hong Kong-Macau Technology Research Programme (Type C) Grant 202108233000303, Hong Kong Research Grants Council (RGC) Collaborative Research Fund (CRF C4026-21GF) 2300075 and (GRS)#3110167.

Institutional Review Board Statement: Not applicable.

Informed Consent Statement: Not applicable.

Data Availability Statement: Not applicable.

Acknowledgments: We would like to acknowledge the CUHK and University of Pittsburgh under CUHK Summer Undergraduate Research Program (SURP)—2022.

Conflicts of Interest: The authors declare no conflict of interest.

References

1. Shampo, M.A.; Kyle, R.A. Karl Theodore Dussik—Pioneer in ultrasound. *Mayo Clin. Proc.* **1995**, *70*, 1136. [[CrossRef](#)] [[PubMed](#)]
2. Wells, P.N.; Liang, H.-D. Medical ultrasound: Imaging of soft tissue strain and elasticity. *J. R. Soc. Interface* **2011**, *8*, 1521–1549. [[CrossRef](#)] [[PubMed](#)]
3. Fenster, A.; Downey, D.B.; Cardinal, H.N. Three-dimensional ultrasound imaging. *Phys. Med. Biol.* **2001**, *46*, R67. [[CrossRef](#)] [[PubMed](#)]
4. Wells, P.N. Ultrasound imaging. *Phys. Med. Biol.* **2006**, *51*, R83. [[CrossRef](#)]
5. Carovac, A.; Smajlovic, F.; Junuzovic, D. Application of ultrasound in medicine. *Acta Inform. Med.* **2011**, *19*, 168–171. [[CrossRef](#)]
6. Szabo, T.L. *Diagnostic Ultrasound Imaging: Inside Out*; Academic Press: Cambridge, MA, USA, 2004.
7. Chan, V.; Perlas, A. Basics of ultrasound imaging. In *Atlas of Ultrasound-Guided Procedures in Interventional Pain Management*; Springer: Berlin/Heidelberg, Germany, 2011; pp. 13–19.
8. Ye, D.; Xue, J.; Yuan, S.; Zhang, F.; Song, S.; Wang, J.; Meng, M.Q.-H. Design and control of a magnetically-actuated capsule robot with biopsy function. *IEEE Trans. Biomed. Eng.* **2022**, *69*, 2905–2915. [[CrossRef](#)]
9. Yuan, S.; Wan, Y.; Song, S. RectMag3D: A magnetic actuation system for steering milli/microrobots based on rectangular electromagnetic coils. *Appl. Sci.* **2020**, *10*, 2677. [[CrossRef](#)]
10. Llamas-Alvarez, A.M.; Tenza-Lozano, E.M.; Latour-Perez, J. Accuracy of lung ultrasonography in the diagnosis of pneumonia in adults: Systematic review and meta-analysis. *Chest* **2017**, *151*, 374–382. [[CrossRef](#)]
11. Powles, A.E.; Martin, D.J.; Wells, I.T.; Goodwin, C.R. Physics of ultrasound. *Anaesth. Intensive Care Med.* **2018**, *19*, 202–205. [[CrossRef](#)]
12. von Haxthausen, F.; Böttger, S.; Wulff, D.; Hagenah, J.; García-Vázquez, V.; Ipsen, S. Medical robotics for ultrasound imaging: Current systems and future trends. *Curr. Robot. Rep.* **2021**, *2*, 55–71. [[CrossRef](#)]
13. Monfaredi, R.; Wilson, E.; Azizi koutenaiei, B.; Labrecque, B.; Leroy, K.; Goldie, J.; Louis, E.; Swerdlow, D.; Cleary, K. Robot-assisted ultrasound imaging: Overview and development of a parallel telerobotic system. *Minim. Invasive Ther. Allied Technol.* **2015**, *24*, 54–62. [[CrossRef](#)] [[PubMed](#)]
14. Baribeau, Y.; Sharkey, A.; Chaudhary, O.; Krumm, S.; Fatima, H.; Mahmood, F.; Matyal, R. Handheld point-of-care ultrasound probes: The new generation of POCUS. *J. Cardiothorac. Vasc. Anesth.* **2020**, *34*, 3139–3145. [[CrossRef](#)] [[PubMed](#)]
15. Aldrich, J.E. Basic physics of ultrasound imaging. *Crit. Care Med.* **2007**, *35*, S131–S137. [[CrossRef](#)]
16. Sigrist, R.M.; Liao, J.; El Kaffas, A.; Chammas, M.C.; Willmann, J.K. Ultrasound elastography: Review of techniques and clinical applications. *Theranostics* **2017**, *7*, 1303–1329. [[CrossRef](#)]
17. Cootney, R.W. Ultrasound imaging: Principles and applications in rodent research. *Ilar J.* **2001**, *42*, 233–247. [[CrossRef](#)]
18. Urone, P.; Hinrichs, R. *College Physics*; OpenStax: Houston, TX, USA, 2012.
19. Abbara, S.; Achenbach, S. *CT and MR in Cardiology*; Elsevier: Amsterdam, The Netherlands, 2019.
20. Wang, J.; Zheng, Z.; Chan, J.; Yeow, J.T. Capacitive micromachined ultrasound transducers for intravascular ultrasound imaging. *Microsyst. Nanoeng.* **2020**, *6*, 1–13. [[CrossRef](#)] [[PubMed](#)]
21. Jiang, Z.; Grimm, M.; Zhou, M.; Esteban, J.; Simson, W.; Zahnd, G.; Navab, N. Automatic normal positioning of robotic ultrasound probe based only on confidence map optimization and force measurement. *IEEE Robot. Autom. Lett.* **2020**, *5*, 1342–1349. [[CrossRef](#)]
22. Giller, C.A.; Giller, A.M. A new method for fixation of probes for transcranial Doppler ultrasound. *J. Neuroimaging* **1997**, *7*, 103–105. [[CrossRef](#)] [[PubMed](#)]
23. Kaczynski, J.; Home, R.; Shields, K.; Walters, M.; Whiteley, W.; Wardlaw, J.; Newby, D.E. Reproducibility of Transcranial Doppler ultrasound in the middle cerebral artery. *Cardiovasc. Ultrasound* **2018**, *16*, 1–10. [[CrossRef](#)]

24. Garami, Z.F.; Bismuth, J.; Charlton-Ouw, K.M.; Davies, M.G.; Peden, E.K.; Lumsden, A.B. Feasibility of simultaneous pre-and postfilter transcranial Doppler monitoring during carotid artery stenting. *J. Vasc. Surg.* **2009**, *49*, 340–345.e342. [[CrossRef](#)]
25. Lao, A.; Sharma, V.; Tsigoulis, G.; Malkoff, M.; Alexandrov, A.; Frey, J. Effect of body positioning during transcranial Doppler detection of right-to-left shunts. *Eur. J. Neurol.* **2007**, *14*, 1035–1039. [[CrossRef](#)] [[PubMed](#)]
26. Kho, E.; Sperna Weiland, N.H.; Vlaar, A.P.; Veelo, D.P.; van der Ster, B.J.; Corsmit, O.T.; Koolbergen, D.R.; Dilai, J.; Immink, R.V. Cerebral hemodynamics during sustained intra-operative hypotension. *J. Appl. Physiol.* **2022**, *132*, 1560–1568. [[CrossRef](#)] [[PubMed](#)]
27. Blans, M.; Bosch, F.; van der Hoeven, J. The use of an external ultrasound fixator (Probefix) on intensive care patients: A feasibility study. *Ultrasound J.* **2019**, *11*, 1–6. [[CrossRef](#)] [[PubMed](#)]
28. Song, I.; Yoon, J.; Kang, J.; Kim, M.; Jang, W.S.; Shin, N.-Y.; Yoo, Y. Design and implementation of a new wireless carotid neckband Doppler system with wearable ultrasound sensors: Preliminary results. *Appl. Sci.* **2019**, *9*, 2202. [[CrossRef](#)]
29. Hettiarachchi, N.; Ju, Z.; Liu, H. A new wearable ultrasound muscle activity sensing system for dexterous prosthetic control. In Proceedings of the 2015 IEEE International Conference on Systems, Man, and Cybernetics, Kowloon Tong, Hong Kong, 9–12 October 2015; pp. 1415–1420.
30. Yang, X.; Chen, Z.; Hettiarachchi, N.; Yan, J.; Liu, H. A wearable ultrasound system for sensing muscular morphological deformations. *IEEE Trans. Man Cybern. Syst.* **2019**, *51*, 3370–3379. [[CrossRef](#)]
31. Yang, X.; Sun, X.; Zhou, D.; Li, Y.; Liu, H. Towards wearable A-mode ultrasound sensing for real-time finger motion recognition. *IEEE Trans. Neural Syst. Rehabil. Eng.* **2018**, *26*, 1199–1208. [[CrossRef](#)]
32. Yang, X.; Yan, J.; Fang, Y.; Zhou, D.; Liu, H. Simultaneous prediction of wrist/hand motion via wearable ultrasound sensing. *IEEE Trans. Neural Syst. Rehabil. Eng.* **2020**, *28*, 970–977. [[CrossRef](#)]
33. Huang, C.-C.; Lee, P.-Y.; Chen, P.-Y.; Liu, T.-Y. Design and implementation of a smartphone-based portable ultrasound pulsed-wave Doppler device for blood flow measurement. *IEEE Trans. Ultrason. Ferroelectr. Freq. Control* **2012**, *59*, 182–188. [[CrossRef](#)]
34. Marugán-Rubio, D.; Chicharro, J.L.; Becerro-de-Bengoa-Vallejo, R.; Losa-Iglesias, M.E.; Rodríguez-Sanz, D.; Vicente-Campos, D.; Dávila-Sánchez, G.J.; Calvo-Lobo, C. Concurrent Validity and Reliability of Manual Versus Specific Device Transcostal Measurements for Breathing Diaphragm Thickness by Ultrasonography in Lumbopelvic Pain Athletes. *Sensors* **2021**, *21*, 4329. [[CrossRef](#)]
35. Nanno, M.; Sawaizumi, T.; Kodera, N.; Tomori, Y.; Takai, S. Ultrasound evaluation of the transverse movement of the flexor pollicis longus tendon on the distal radius during wrist and finger motion in healthy volunteers. *J. Nippon. Med. Sch.* **2015**, *82*, 220–228. [[CrossRef](#)]
36. Nanno, M.; Kodera, N.; Tomori, Y.; Hagiwara, Y.; Takai, S. Median nerve movement in the carpal tunnel before and after carpal tunnel release using transverse ultrasound. *J. Orthop. Surg.* **2017**, *25*, 2309499017730422. [[CrossRef](#)]
37. Heres, H.M.; Sjoerdsma, M.; Schoots, T.; Rutten, M.; van de Vosse, F.N.; Lopata, R.G. Image acquisition stability of fixated musculoskeletal sonography in an exercise setting: A quantitative analysis and comparison with freehand acquisition. *J. Med. Ultrason.* **2020**, *47*, 47–56. [[CrossRef](#)] [[PubMed](#)]
38. Shih, Y.-F.; Bull, A.M.; McGregor, A.H.; Amis, A.A. Active patellar tracking measurement: A novel device using ultrasound. *Am. J. Sport. Med.* **2004**, *32*, 1209–1217. [[CrossRef](#)] [[PubMed](#)]
39. Molyneux, P.; Ellis, R.F.; Carroll, M. Reliability of a two-probe ultrasound imaging procedure to measure strain in the Achilles tendon. *J. Foot Ankle Res.* **2019**, *12*, 1–9. [[CrossRef](#)] [[PubMed](#)]
40. Sjoerdsma, M.; Caresio, C.; Tchang, B.; Meeder, A.; van de Vosse, F.; Lopata, R. The feasibility of dynamic musculoskeletal function analysis of the vastus lateralis in endurance runners using continuous, hands-free ultrasound. *Appl. Sci.* **2021**, *11*, 1534. [[CrossRef](#)]
41. Kim, J.; Lee, S. Development of a wearable robotic positioning system for noninvasive transcranial focused ultrasound stimulation. *IEEE/ASME Trans. Mechatron.* **2016**, *21*, 2284–2293. [[CrossRef](#)]
42. Ren, H.; Gu, X.; Tan, K.L. Human-compliant body-attached soft robots towards automatic cooperative ultrasound imaging. In Proceedings of the 2016 IEEE 20th International Conference on Computer Supported Cooperative Work in Design (CSCWD), Nanchang, China, 4–6 May 2016; pp. 653–658.
43. Li, L.; Long, F.L.J.; Lim, I.; Sun, T.; Ren, H. An Overhead Collapsible Origami-Based Mount for Medical Applications. *Robotics* **2023**, *12*, 21. [[CrossRef](#)]
44. Zeiler, F.A.; Czosnyka, M.; Smielewski, P. Optimal cerebral perfusion pressure via transcranial Doppler in TBI: Application of robotic technology. *Acta Neurochir.* **2018**, *160*, 2149–2157. [[CrossRef](#)]
45. Zeiler, F.; Smielewski, P. Application of robotic transcranial Doppler for extended duration recording in moderate/severe traumatic brain injury: First experiences. *Crit. Ultrasound J.* **2018**, *10*, 1–8. [[CrossRef](#)]
46. Khan, D.Z.; Placek, M.M.; Smielewski, P.; Budohoski, K.P.; Anwar, F.; Hutchinson, P.J.; Bance, M.; Czosnyka, M.; Helmy, A. Robotic semi-automated transcranial doppler assessment of cerebrovascular autoregulation in post-concussion syndrome: Methodological considerations. *Neurotrauma Rep.* **2020**, *1*, 218–231. [[CrossRef](#)]
47. Krakauskaite, S.; Kumpaitiene, B.; Svagzdiene, M.; Sirvinskas, E.; Petkus, V.; Chaleckas, E.; Kasputyte, G.; Gailiusas, M.; Benetis, R.; Ragauskas, A. Non-invasive Intracranial Pressure Dynamics During Cardiac Bypass Surgery: Prospective Study. In Proceedings of the 12th International Conference on Biomedical Engineering and Technology, Tokyo, Japan, 15–18 June 2023; pp. 175–179.

48. Pizzarelli, G.; Gennai, S.; Leone, N.; Covic, T.; Moratto, R.; Silingardi, R. Transcranial Doppler detects micro emboli in patients with asymptomatic carotid stenoses undergoing endarterectomy. *J. Vasc. Surg.* **2022**, *77*, 811–817. [[CrossRef](#)]
49. Aarli, S.J.; Novotny, V.; Thomassen, L.; Kvistad, C.E.; Logallo, N.; Fromm, A. Persistent microembolic signals in the cerebral circulation on transcranial Doppler after intravenous sulfur hexafluoride microbubble infusion. *J. Neuroimaging* **2020**, *30*, 146–149. [[CrossRef](#)]
50. Thorpe, S.G.; Thibeault, C.M.; Wilk, S.J.; O'Brien, M.; Canac, N.; Ranjbaran, M.; Devlin, C.; Devlin, T.; Hamilton, R.B. Velocity curvature index: A novel diagnostic biomarker for large vessel occlusion. *Transl. Stroke Res.* **2019**, *10*, 475–484. [[CrossRef](#)] [[PubMed](#)]
51. Overman, D. FDA Clears iSono Health's ATUSA, an Automated and Wearable 3D Breast Ultrasound System. Available online: <https://axisimagingnews.com/radiology-products/imaging-equipment/ultrasound/fda-clears-isono-healths-atusa-an-automated-and-wearable-3d-breast-ultrasound-system> (accessed on 22 February 2023).
52. van Leuteren, P.G.; Klijn, A.J.; de Jong, T.P.; Dik, P. SENS-U: Validation of a wearable ultrasonic bladder monitor in children during urodynamic studies. *J. Pediatr. Urol.* **2018**, *14*, 569.e561–569.e566. [[CrossRef](#)] [[PubMed](#)]
53. Kwinten, W.; van Leuteren, P.; van Duren-van Iersel, M.; Dik, P.; Jira, P. SENS-U: Continuous home monitoring of natural nocturnal bladder filling in children with nocturnal enuresis—a feasibility study. *J. Pediatr. Urol.* **2020**, *16*, 196.e191–196.e196. [[CrossRef](#)] [[PubMed](#)]
54. van Leuteren, P.G.; Nieuwhof-Leppink, A.J.; Dik, P. SENS-U: Clinical evaluation of a full-bladder notification—a pilot study. *J. Pediatr. Urol.* **2019**, *15*, 381.e381–381.e385. [[CrossRef](#)] [[PubMed](#)]
55. La, T.G.; Le, L.H. Flexible and wearable ultrasound device for medical applications: A review on materials, structural designs, and current challenges. *Adv. Mater. Technol.* **2022**, *7*, 2100798. [[CrossRef](#)]
56. Awad, E. Design of a Wearable Ultrasound Doppler Sensor to Monitor Blood Flow in the Common Carotid Artery. Ph.D. Dissertation, Massachusetts Institute of Technology, Cambridge, MA, USA, 1999.
57. Awad, E.; Asada, H. The Doppler necklace: A wearable and noninvasive ultrasound sensor for continuous monitoring of blood flow in the common carotid artery. In Proceedings of the First Joint BMES/EMBS Conference. 1999 IEEE Engineering in Medicine and Biology 21st Annual Conference and the 1999 Annual Fall Meeting of the Biomedical Engineering Society, Atlanta, GA, USA, 13–16 October 1999; Volume 792, p. 795.
58. AlMohimeed, I.; Turkistani, H.; Ono, Y. Development of wearable and flexible ultrasonic sensor for skeletal muscle monitoring. In Proceedings of the 2013 IEEE International Ultrasonics Symposium (IUS), Prague, Czech Republic, 21–25 July 2013; pp. 1137–1140.
59. AlMohimeed, I. Development of Wearable Ultrasonic Sensors for Monitoring Muscle Contraction. Master Thesis, Carleton University, Ottawa, ON, Canada, 2013.
60. Liu, W.; Zhu, C.; Wu, D. Flexible piezoelectric micro ultrasonic transducer array integrated on various flexible substrates. *Sens. Actuators A Phys.* **2021**, *317*, 112476. [[CrossRef](#)]
61. Hu, H. Continuous Monitoring of Deep Tissue with a Stretchable Ultrasonic Patch. Ph.D. Dissertation, UC San Diego, La Jolla, CA, USA, 2021.
62. Hu, H.; Zhu, X.; Wang, C.; Zhang, L.; Li, X.; Lee, S.; Huang, Z.; Chen, R.; Chen, Z.; Wang, C. Stretchable ultrasonic transducer arrays for three-dimensional imaging on complex surfaces. *Sci. Adv.* **2018**, *4*, eaar3979. [[CrossRef](#)]
63. Sempionatto, J.R.; Lin, M.; Yin, L.; Pei, K.; Sonsa-ard, T.; de Loyola Silva, A.N.; Khorshed, A.A.; Zhang, F.; Tostado, N.; Xu, S. An epidermal patch for the simultaneous monitoring of haemodynamic and metabolic biomarkers. *Nat. Biomed. Eng.* **2021**, *5*, 737–748. [[CrossRef](#)]
64. Wang, C.; Qi, B.; Lin, M.; Zhang, Z.; Makihata, M.; Liu, B.; Zhou, S.; Huang, Y.-h.; Hu, H.; Gu, Y. Continuous monitoring of deep-tissue haemodynamics with stretchable ultrasonic phased arrays. *Nat. Biomed. Eng.* **2021**, *5*, 749–758. [[CrossRef](#)] [[PubMed](#)]
65. Pashaei, V.; Dehghanzadeh, P.; Enwia, G.; Bayat, M.; Majerus, S.J.; Mandal, S. Flexible body-conformal ultrasound patches for image-guided neuromodulation. *IEEE Trans. Biomed. Circuits Syst.* **2019**, *14*, 305–318. [[CrossRef](#)] [[PubMed](#)]
66. Wang, C.; Chen, X.; Wang, L.; Makihata, M.; Liu, H.-C.; Zhou, T.; Zhao, X. Bioadhesive ultrasound for long-term continuous imaging of diverse organs. *Science* **2022**, *377*, 517–523. [[CrossRef](#)] [[PubMed](#)]
67. Nuckols, R.W.; Lee, S.; Swaminathan, K.; Orzel, D.; Howe, R.D.; Walsh, C.J. Individualization of exosuit assistance based on measured muscle dynamics during versatile walking. *Sci. Robot.* **2021**, *6*, eabj1362. [[CrossRef](#)] [[PubMed](#)]
68. Bhuyan, A.; Choe, J.W.; Lee, B.C.; Cristman, P.; Oralkan, Ö.; Khuri-Yakub, B.T. Miniaturized, wearable, ultrasound probe for on-demand ultrasound screening. In Proceedings of the 2011 IEEE International Ultrasonics Symposium, Orlando, FL, USA, 18–21 October 2011; pp. 1060–1063.
69. Kenny, J.-É.S.; Munding, C.E.; Eibl, J.K.; Eibl, A.M.; Long, B.F.; Boyes, A.; Yin, J.; Verrecchia, P.; Parrotta, M.; Gatzke, R. A novel, hands-free ultrasound patch for continuous monitoring of quantitative Doppler in the carotid artery. *Sci. Rep.* **2021**, *11*, 1–11. [[CrossRef](#)]
70. Kenny, J.-É.S. Functional hemodynamic monitoring with a wireless ultrasound patch. *J. Cardiothorac. Vasc. Anesth.* **2021**, *35*, 1509–1515. [[CrossRef](#)] [[PubMed](#)]
71. Munding, C.; Acconcia, C.; Elfarnawany, M.; Eibl, J.; Verrecchia, P.; Leonard, P.; Boyes, A.; Yang, Z.; Atoui, R.; Demore, C. In vitro and clinical demonstration of relative velocity measurements with the Flopatch™: A wearable Doppler ultrasound patch. In Proceedings of the 2021 IEEE International Ultrasonics Symposium (IUS), Xi'an, China, 11–16 September 2021; pp. 1–4.

72. Kenny, J.-É.S.; Clarke, G.; Myers, M.; Elfarnawany, M.; Eibl, A.M.; Eibl, J.K.; Nalla, B.; Atoui, R. A wireless wearable doppler ultrasound detects changing stroke volume: Proof-of-Principle comparison with trans-esophageal echocardiography during coronary bypass surgery. *Bioengineering* **2021**, *8*, 203. [[CrossRef](#)]
73. Gerardo, C.D.; Cretu, E.; Rohling, R. Fabrication and testing of polymer-based capacitive micromachined ultrasound transducers for medical imaging. *Microsyst. Nanoeng.* **2018**, *4*, 1–12. [[CrossRef](#)]
74. Omidvar, A.; Gerardo, C.D.; Rohling, R.; Cretu, E.; Hodgson, A.J. Flexible polymer-based capacitive micromachined ultrasound transducers (polyCMUTs): Fabrication and characterization. In Proceedings of the 2021 IEEE International Ultrasonics Symposium (IUS), Xi'an, China, 11–16 September 2021; pp. 1–4.
75. Gerardo, C.D.; Cretu, E.; Rohling, R. Fabrication of circuits on flexible substrates using conductive SU-8 for sensing applications. *Sensors* **2017**, *17*, 1420. [[CrossRef](#)]
76. Tuysuzoglu, A.; Tan, J.; Eissa, K.; Kiraly, A.P.; Diallo, M.; Kamen, A. Deep adversarial context-aware landmark detection for ultrasound imaging. In Proceedings of the International Conference on Medical Image Computing and Computer-Assisted Intervention, Granada, Spain, 16–20 September 2018; pp. 151–158.
77. Li, H.; Weng, J.; Shi, Y.; Gu, W.; Mao, Y.; Wang, Y.; Liu, W.; Zhang, J. An improved deep learning approach for detection of thyroid papillary cancer in ultrasound images. *Sci. Rep.* **2018**, *8*, 1–12. [[CrossRef](#)]
78. Diamant, A.; Chatterjee, A.; Vallières, M.; Shenouda, G.; Seuntjens, J. Deep learning in head & neck cancer outcome prediction. *Sci. Rep.* **2019**, *9*, 1–10.
79. Chao, P.C.-P.; Chiang, P.-Y.; Kao, Y.-H.; Tu, T.-Y.; Yang, C.-Y.; Tarng, D.-C.; Wey, C.-L. A portable, wireless photoplethysmography sensor for assessing health of arteriovenous fistula using class-weighted support vector machine. *Sensors* **2018**, *18*, 3854. [[CrossRef](#)]
80. Zhao, X.; Zeng, X.; Koehl, L.; Tartare, G.; De Jonckheere, J. A wearable system for in-home and long-term assessment of fetal movement. *IRBM* **2020**, *41*, 205–211. [[CrossRef](#)]
81. Mesbah, M.; Khlif, M.S.; Layeghy, S.; East, C.E.; Dong, S.; Brodtmann, A.; Colditz, P.B.; Boashash, B. Automatic fetal movement recognition from multi-channel accelerometry data. *Comput. Methods Programs Biomed.* **2021**, *210*, 106377. [[CrossRef](#)]
82. Willeminck, M.J.; Koszek, W.A.; Hardell, C.; Wu, J.; Fleischmann, D.; Harvey, H.; Folio, L.R.; Summers, R.M.; Rubin, D.L.; Lungren, M.P. Preparing medical imaging data for machine learning. *Radiology* **2020**, *295*, 4–15. [[CrossRef](#)] [[PubMed](#)]
83. Basak, A.; Ranganathan, V.; Bhunia, S. A wearable ultrasonic assembly for point-of-care autonomous diagnostics of malignant growth. In Proceedings of the 2013 IEEE Point-of-Care Healthcare Technologies (PHT), Bangalore, India, 16–18 January 2013; pp. 128–131.
84. Hou, D.; Hou, R.; Hou, J. On-device Training for Breast Ultrasound Image Classification. In Proceedings of the 2020 10th Annual Computing and Communication Workshop and Conference (CCWC), Las Vegas, NV, USA, 6–8 January 2020; pp. 0078–0082.
85. Mnih, V.; Kavukcuoglu, K.; Silver, D.; Rusu, A.A.; Veness, J.; Bellemare, M.G.; Graves, A.; Riedmiller, M.; Fidjeland, A.K.; Ostrovski, G. Human-level control through deep reinforcement learning. *Nature* **2015**, *518*, 529–533. [[CrossRef](#)] [[PubMed](#)]
86. Chen, Y.F.; Everett, M.; Liu, M.; How, J.P. Socially aware motion planning with deep reinforcement learning. In Proceedings of the 2017 IEEE/RSJ International Conference on Intelligent Robots and Systems (IROS), Vancouver, BC, Canada, 24–28 September 2017; pp. 1343–1350.
87. Yuan, W.; Stork, J.A.; Kragic, D.; Wang, M.Y.; Hang, K. Rearrangement with nonprehensile manipulation using deep reinforcement learning. In Proceedings of the 2018 IEEE International Conference on Robotics and Automation (ICRA), Brisbane, QLD, Australia, 21–25 May 2018; pp. 270–277.
88. Burke, M.; Lu, K.; Angelov, D.; Straižys, A.; Innes, C.; Subr, K.; Ramamoorthy, S. Learning rewards for robotic ultrasound scanning using probabilistic temporal ranking. *arXiv* **2020**, arXiv:2002.01240.
89. Droste, R.; Drukker, L.; Papageorgiou, A.T.; Noble, J.A. Automatic probe movement guidance for freehand obstetric ultrasound. In Proceedings of the International Conference on Medical Image Computing and Computer-Assisted Intervention, Lima, Peru, 4–8 October 2020; pp. 583–592.
90. Jarosik, P.; Lewandowski, M. Automatic ultrasound guidance based on deep reinforcement learning. In Proceedings of the 2019 IEEE International Ultrasonics Symposium (IUS), Glasgow, UK, 6–9 October 2019; pp. 475–478.
91. Milletari, F.; Birodar, V.; Sofka, M. Straight to the point: Reinforcement learning for user guidance in ultrasound. In *Smart Ultrasound Imaging and Perinatal, Preterm and Paediatric Image Analysis*; Springer: Berlin/Heidelberg, Germany, 2019; pp. 3–10.
92. Sharifrazi, D.; Alizadehsani, R.; Roshanzamir, M.; Joloudari, J.H.; Shoeibi, A.; Jafari, M.; Hussain, S.; Sani, Z.A.; Hasanzadeh, F.; Khozimeh, F. Fusion of convolution neural network, support vector machine and Sobel filter for accurate detection of COVID-19 patients using X-ray images. *Biomed. Signal Process. Control* **2021**, *68*, 102622. [[CrossRef](#)]
93. Oh, S.L.; Jahmunah, V.; Ooi, C.P.; Tan, R.-S.; Ciaccio, E.J.; Yamakawa, T.; Tanabe, M.; Kobayashi, M.; Acharya, U.R. Classification of heart sound signals using a novel deep WaveNet model. *Comput. Methods Programs Biomed.* **2020**, *196*, 105604. [[CrossRef](#)]
94. Zhao, L.; Li, K.; Pu, B.; Chen, J.; Li, S.; Liao, X. An ultrasound standard plane detection model of fetal head based on multi-task learning and hybrid knowledge graph. *Future Gener. Comput. Syst.* **2022**, *135*, 234–243. [[CrossRef](#)]
95. Kuo, C.-C.; Chang, C.-M.; Liu, K.-T.; Lin, W.-K.; Chiang, H.-Y.; Chung, C.-W.; Ho, M.-R.; Sun, P.-R.; Yang, R.-L.; Chen, K.-T. Automation of the kidney function prediction and classification through ultrasound-based kidney imaging using deep learning. *NPJ Digit. Med.* **2019**, *2*, 1–9. [[CrossRef](#)] [[PubMed](#)]
96. Hu, Y.; Guo, Y.; Wang, Y.; Yu, J.; Li, J.; Zhou, S.; Chang, C. Automatic tumor segmentation in breast ultrasound images using a dilated fully convolutional network combined with an active contour model. *Med. Phys.* **2019**, *46*, 215–228. [[CrossRef](#)] [[PubMed](#)]

97. Lu, Y.; Li, J.; Zhao, X.; Li, J.; Feng, J.; Fan, E. Breast cancer research and treatment reconstruction of unilateral breast structure using three-dimensional ultrasound imaging to assess breast neoplasm. *Breast Cancer Res. Treat.* **2019**, *176*, 87–94. [[CrossRef](#)] [[PubMed](#)]
98. Zhang, J.; He, Q.; Xiao, Y.; Zheng, H.; Wang, C.; Luo, J. Ultrasound image reconstruction from plane wave radio-frequency data by self-supervised deep neural network. *Med. Image Anal.* **2021**, *70*, 102018. [[CrossRef](#)]
99. Gupta, M.; Taneja, H.; Chand, L. Performance enhancement and analysis of filters in ultrasound image denoising. *Procedia Comput. Sci.* **2018**, *132*, 643–652. [[CrossRef](#)]
100. Thring, C.; Band, F.; Irving, D.; McAughey, K.; Hughes, D.A. Novel, High Temperature, Low Frequency, Thin Film, NDT Ultrasound Transducers. In Proceedings of the 2020 IEEE International Ultrasonics Symposium (IUS), Las Vegas, NV, USA, 7–11 September 2020; pp. 1–3.
101. Lammie, C.; Xiang, W.; Azghadi, M.R. Towards memristive deep learning systems for real-time mobile epileptic seizure prediction. In Proceedings of the 2021 IEEE International Symposium on Circuits and Systems (ISCAS), Daegu, Republic of Korea, 22–28 May 2021; pp. 1–5.
102. Zhu, J.; Zhang, S.; Yu, R.; Liu, Z.; Gao, H.; Yue, B.; Liu, X.; Zheng, X.; Gao, M.; Wei, X. An efficient deep convolutional neural network model for visual localization and automatic diagnosis of thyroid nodules on ultrasound images. *Quant. Imaging Med. Surg.* **2021**, *11*, 1368. [[CrossRef](#)]
103. Pesteie, M.; Lessoway, V.; Abolmaesumi, P.; Rohling, R.N. Automatic localization of the needle target for ultrasound-guided epidural injections. *IEEE Trans. Med. Imaging* **2017**, *37*, 81–92. [[CrossRef](#)]

Disclaimer/Publisher’s Note: The statements, opinions and data contained in all publications are solely those of the individual author(s) and contributor(s) and not of MDPI and/or the editor(s). MDPI and/or the editor(s) disclaim responsibility for any injury to people or property resulting from any ideas, methods, instructions or products referred to in the content.